Equilibrium Vacancy Concentration Measurements on Solid Krypton*

D. L. Losee† and R. O. Simmons
Department of Physics and Materials Research Laboratory, University of Illinois, Urbana, Illinois
(Received 4 April 1968)

Simultaneous length and x-ray lattice-parameter expansion measurements have been made on 6-mm-diam cylindrical specimens of 99.99%-purity krypton. The specimens were prepared and held in a rigid-tail cryostat in which specimen temperatures could be precisely controlled. The data show a divergence between the bulk and x-ray expansions at the higher temperatures, which indicates an appreciable net concentration of thermally generated vacancy defects at temperatures above 75°K. The equilibrium atomic-vacancy concentration inferred from these measurements may be represented by $\exp[(2.0_{-0.5}^{+1.0}) - (895\pm100)\,°\mathrm{K}/T]$. The monovacancy formation enthalpy and entropy are discussed and compared with other existing theoretical and experimental information on argon and krypton. From the present direct measurements it appears that the enthalpy of formation for the monovacancy in krypton may not be entirely accounted for by two-body central-force interactions. However, existing calculations of the contribution of many-body interactions to the binding energy of the noble-gas solids appear to be of the correct order of magnitude and sign to improve agreement between theory and experiment for the vacancy. It is found that an empirical law of corresponding states which describes a number of the bulk thermal properties of the noble-gas solids may also describe some of the defect properties.

ATOMS of the noble gases are characterized by closed electronic shells, spherical symmetry, and weak interatomic forces. In the solid state, these elements, with helium as an exception, condense into the fcc structure. These characteristics have encouraged the hope that one might be able to predict in detail, from first principles, the properties of the noble-gas solids. However, because of the difficulties involved in the preparation and handling of suitable specimens, relatively few experiments have been performed which may be critically compared with theory. Several authors[1] have reviewed selected aspects of existing experimental and theoretical knowledge of these solids.

The dominant thermal defect in close-packed solids is the atomic vacancy. For the noble-gas solids, numerous calculations of vacancy properties have been made.[2–14] However, predictions of vacancy concentration, entropy, energy, and volume of formation have varied considerably, thus pointing out the need for experimental evidence. Vacancies in these crystals have intrinsic interest as prototypes upon which first-principle studies of rate processes in solids might be carried out. It is also possible that comparison between theory and experiment for the vacancy can yield rather direct information about the importance of many-body interatomic forces in insulating crystals.[5,6,15]

Of all the noble-gas solids, krypton seems to be the most appropriate and interesting for making an initial direct defect concentration measurement, because of its relatively high triple-point temperature and the availability of accurate calorimetric data.[16] The large mass of the krypton atom should keep quantum zero-point effects small in any theoretical calculations.

In principle, the most direct measurement of net vacancy concentration is through the use of the relation

$$\Delta N/N=(V-V_x)/V_x, \tag{1}$$

where $\Delta N/N$ is the net added concentration of substitutional atomic sites in a crystal containing N atoms. V is the bulk volume and V_x is the volume as determined by x-ray diffraction. For a fcc crystal $V_x=\frac{1}{4}Na^3$, where a is the lattice constant. However, the most reliable way of determining vacancy concentrations in practice is to make simultaneous measurements of changes with temperature in the bulk and x-ray volumes, or, equivalently, to measure changes in linear dimension and in lattice parameter of the specimen.[17] In the latter case, one has for a cubic crystal

$$\Delta N/N=3(\Delta l/l_0-\Delta a/a_0), \tag{2}$$

* Work supported in part by U. S. Atomic Energy Commission under Contract No. AT(11-1)-1198, Report No. C00-1198-459.

† U. S. National Aeronautics and Space Administration Trainee, 1963–1966. Present address: Eastman Kodak Research Laboratory, Rochester, N. Y. This paper is based in part on the Ph.D. thesis presented by D.L.L. at the University of Illinois, Urbana, Ill.

[1] E. R. Dobbs and G. O. Jones, Rept. Progr. Phys. **20**, 516 (1957); A. C. Hallett, in *Argon, Helium, and the Rare Gases*, edited by G. A. Cook (Interscience Publishers, Inc., New York, 1961), Vol. I, p. 313; G. L. Pollack, Rev. Mod. Phys. **36**, 748 (1964); G. Boato, Cryogenics **4**, 65 (1964); G. K. Horton, Am. J. Phys. **36**, 93 (1968).

[2] H. Kanzaki, J. Phys. Chem. Solids **2**, 24 (1957).

[3] G. L. Hall, J. Phys. Chem. Solids **3**, 210 (1957).

[4] G. F. Nardelli and A. Chiarotti, Nuovo Cimento **18**, 1053 (1960).

[5] L. Jansen, Phil. Mag. **8**, 1305 (1963).

[6] A. J. E. Foreman, Phil. Mag. **8**, 1211 (1963).

[7] R. Fieschi, G. F. Nardelli, and A. R. Chiarotti, Phys. Rev. **123**, 141 (1963).

[8] V. Gallina and M. Omini, Phys. Status Solidi **6**, 391 (1964); **6**, 627 (1964).

[9] G. F. Nardelli and N. Terzi, J. Phys. Chem. Solids **25**, 815 (1964).

[10] S. Doniach and R. Huggins, Phil. Mag. **12**, 393 (1965).

[11] J. J. Burton and G. Jura, J. Phys. Chem. Solids **27**, 961 (1966); **28**, 705 (1967).

[12] H. R. Glyde, J. Phys. Chem. Solids **27**, 1659 (1966); Rev. Mod. Phys. **39**, 373 (1967).

[13] R. M. J. Cotterill and M. Doyama, Phys. Letters **25A**, 35 (1967).

[14] K. Mukherjee, Phys. Letters **25A**, 439 (1967).

[15] D. L. Losee and R. O. Simmons, Phys. Rev. Letters **18**, 451 (1967). This is a preliminary report of the present measurements.

[16] R. H. Beaumont H. Chihara, and J. A. Morrison, Proc. Phys. Soc. (London) **78**, 1462 (1961).

[17] R. O. Simmons, in *Rendiconti della Scuola International de Fisica "E. Fermi"—XVIII Corso*, edited by D. S. Billington (Academic Press Inc., New York, 1962), p. 568. Extensive direct work on fcc metals is cited in D. R. Beaman, R. W. Balluffi, and R. O. Simmons, Phys. Rev. **137**, A917 (1965); and earlier papers.

where l_0 and a_0 are a reference length and lattice parameter, respectively, measured at a temperature where there is a negligible thermal defect concentration. Δl and Δa are the changes in these quantities measured at higher temperatures. This method is independent of the state of aggregation of the atomic defects, is independent of information or assumption concerning the detailed lattice relaxation in the immediate neighborhood of the defects, and is insensitive to the presence of voids or microporosity. We have applied this method in the present work.

I. EXPERIMENTAL METHOD

In applying Eq. (2) it is important to observe several experimental precautions. First, the temperature scales for the length and lattice-parameter measurements must be the same because of thermal expansion. Second, the specimens used for the two measurements must be of the same composition since different impurity contents may change both defect concentrations and thermal expansivities. The best way to avoid these difficulties is to make the length and lattice-parameter measurements simultaneously on the same specimen.

Length-change measurements must be made on an unconstrained specimen where the absence of creep or plastic deformation is ensured. The sources and sinks for the thermal defects are primarily at dislocations and internal crystal sub-boundaries. These may conceivably be arranged in some anisotropic manner in a particular specimen, leading to violation of the bulk relation $\Delta V/V_0=3\Delta l/l_0$. In the data used in this paper, there is no evidence contrary to an assumption of isotropic source and sink action.

To apply this method of defect concentration measurement to the noble-gas solids, one is faced with additional difficulties due to low melting points, extremely low yield strengths at the higher temperatures where vacancies are present, severe brittleness at lower temperatures, and firm adhesion of the solids to all materials used to construct cryostat parts. The vapor pressures of the noble-gas solids are extremely high near the melting point, for example, about 0.7 bar in krypton at the triple point. High vapor pressure may lead to substantial mass transport if temperature inhomogeneities are present. Further, it renders specimen surface features unstable.

The experimental method used in the present research attempted to minimize the considerable difficulties mentioned above. Figure 1 schematically illustrates the arrangement employed in making the necessary precise length and lattice-parameter measurements. Solid krypton specimens were prepared in place and were never moved.

A. Specimen Chamber and Temperature Control

The heavy copper specimen chamber is shown in cutaway view in Fig. 2. Three thin-wall Inconel posts

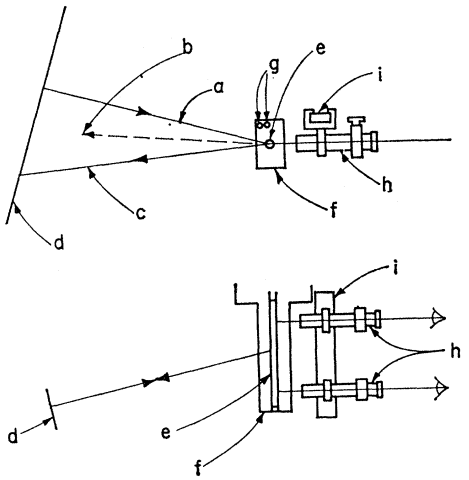

FIG. 1. Schematic diagram of length and lattice-parameter measurement apparatus. Both $\Delta l/l_0$ and $\Delta a/a_0$ are measured absolutely. Incident x-ray beam a is diffracted by crystal lattice planes with normal b. Diffracted beam c darkens film at d; the x-ray source and film are rotated together at a uniform angular rate. The specimen e is maintained in cryostat tail f and temperature is measured by resistance thermometers g. Length-change measurements are made by visual observation, of markers embedded within the specimen, through 100× filar micrometer microscopes h, held at fixed separation on Invar bar i.

provided firm yet thermally insulating support for the specimen chamber below the rigid helium reservoir tail, similar to the arrangement described by Peterson and Simmons.[18] A fluid helium-flow system employed a spiral-tube heat exchanger on the upper part of the chamber. In the present cryostat, a more extensive system of nickel-plated heat shields was incorporated around the chamber in order to ensure the necessary homogeneity of temperature over the krypton specimen length of about 11 cm. The optical windows were Corning Type I-69 filters, which have negligible transmission beyond 3-μm wavelength. The specimen-chamber vacuum was independent of the main Dewar vacuum.

The extra-thick left wall of the specimen chamber housed the strain-free, NBS-calibrated, germanium and platinum resistance thermometers. Thermometer resistance changes served as input to a feedback circuit which produced an appropriate change in the current flow through a 200-Ω heater evenly distributed over the specimen-chamber surface and held there by epoxy resin. During measurements, the temperature control system provided better than ± 0.01°K regulation for all temperatures above 20°K. During specimen growth, over periods of a week or more, temperature fluctuations were less than ± 0.1°K.

A series of measurements made on a phenolic dummy specimen of appropriate thermal conduction, with thermocouples embedded along its length, revealed no significant temperature gradient along the length of the specimen under usual $\Delta l/l_0$ and $\Delta a/a_0$ measurement

[18] O. G. Peterson and R. O. Simmons, Rev. Sci. Instr. 36, 1316 (1965).

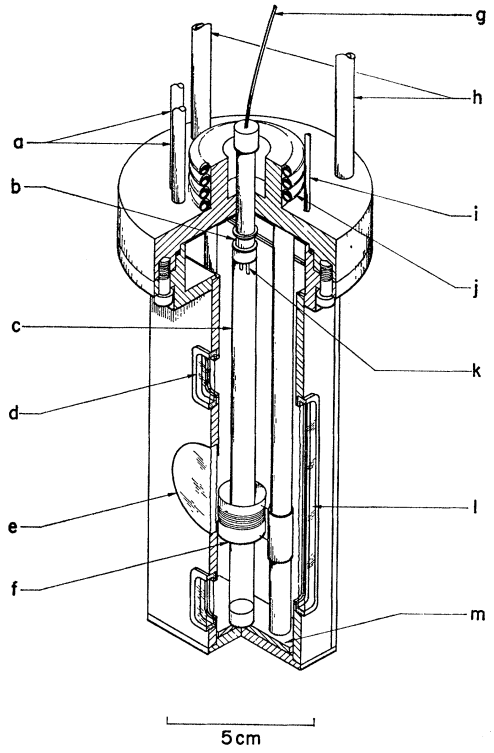

FIG. 2. Cutaway view of specimen chamber, which provides for krypton crystal growth and subsequently holds the specimen at a fixed uniform temperature during each measurement. a: Conduit for electrical leads. b: Heater. c: Mylar specimen tube. d: One of the four heat-absorbing glass windows to permit length measurement in transmitted light. e: 1-mm-thick beryllium x-ray window. f: Movable heater. g: Capillary for sample gas. h: Inconel support posts. i: Conduit for nylon monofilament to control position of heater f. j: Copper heat exchanger coil to bring fluid helium from reservoir at controlled rate. k: Electromagnet to hold specimen markers. l: Heat-absorbing window for observation of crystal growth and alignment of x-ray camera. m: Copper plate. The entire chamber is surrounded by a radiation shield at a lower temperature.

conditions. This evidence and the excellent agreement between the bulk and x-ray expansions measured over a large range of lower temperatures indicate that the average temperature along the length of the specimen closely agrees with the temperature of the x-rayed portion of the specimen. The possible heating effect of the incident x-ray beam proved to be negligible as evidenced by lattice-parameter measurements made at elevated temperatures using a wide range of incident x-ray intensities.

B. Specimen Preparation and Handling

All specimens were prepared from "research-grade" krypton supplied by the Matheson Co. Lot analysis of the gas showed less than 25 ppm nitrogen as the principal impurity, all other impurities being undetected. The preparation scheme described below may have added a small amount of helium to each specimen by diffusion. We estimate this added helium to be only a few ppm.

A 0.025-mm-thick, 6.4-mm-diam tube constructed of Mylar sheet, rolled into cylindrical shape and fastened with epoxy resin, was the "crucible" for a Bridgman crystal-growth scheme. Copper plugs sealed the top and bottom of the specimen tube and a capillary tube admitted the sample gas (see Fig. 2).

With the specimen chamber slightly above the triple-point temperature (115.8°K), krypton gas was admitted to the specimen tube and liquified. The specimen tube could then be sealed off after being filled with liquid. Lowering the sample-chamber temperature to a point a few tenths of a degree below the triple point allowed solidification to begin. Surrounding the Mylar "crucible", a 100-Ω movable heater or "furnace" traveled along two copper guide posts. Through variation of the position and power of this movable heater, precise control of the specimen growth was possible. Directional solidification proceeded at a slow rate, usually between 0.3 and 0.5 mm/h. Generally, the liquid-solid interface was very flat (radius of curvature >10 cm), indicating a uniform vertical temperature gradient.

Four small electromagnets were located at the top inside of the specimen tube. These magnets served to hold and then to release the spherical steel markers (50 μm average diameter) which were embedded within each specimen during solidification. At all times during the crystal-growth process the specimen chamber was evacuated. After the completion of solidification, about 1-Torr helium exchange gas, admitted to the specimen chamber outside the specimen tube, removed any residual temperature inhomogeneities.

By slight reduction of the vapor pressure over the solid, the specimen could be separated from the walls of the Mylar tube. This "thermal-etching" process allowed visual examination of the specimen crystal quality and clearly revealed any grain boundaries which might exist. Moreover, the separation prevented subsequent deformation of the fragile specimen surface during cooling. Specimens consisted of three or four major crystals, sometimes with a few smaller crystals at the unused extremities of the specimen. Grain boundaries which were nearly horizontal resulted from the careful maintenance of the vertical temperature gradient during solidification.

To cool the specimen after the separation from the Mylar tube it was necessary to reevacuate the specimen chamber and cool the specimen by conduction through its lower end. Extremely slow cooling rates are necessary for this method, less than 0.5°K/h, in order to avoid a large degree of mass transport of solid to the colder end of the specimen via the vapor phase. Cooling from the triple point was stopped at intervals to reseparate the specimen from the Mylar tube. After the last separation, a small amount of vapor-deposited solid at the very

bottom of the specimen served to cement the specimens in place, free of any contact with the specimen tube over the entire upper portion.

The same considerations noted above regarding rates of temperature change also apply on heating, though to a lesser degree. The number of temperature cycles to check reversibility for a given specimen was therefore limited because of the slow irreversible changes in the specimen surface, and hence marker appearance, as noted below.

C. Length-Change Measurements

The instability of the surfaces of the noble-gas solids at high temperature eliminates the use of any method of length measurement primarily dependent on surface conditions. Since the noble-gas solids are transparent, length measurements could be made by observing the positions of spherical steel markers embedded a short distance beneath the specimen surface. The 50-μm-diam markers were small enough to ensure negligible effect due to stresses around them. Such stresses could arise either through differential thermal contraction or through gravitational force on the dense markers.

The Invar bar supporting the microscopes (see Fig. 2) could be precisely translated and rotated to allow the observer to measure accurately the true separation between chosen markers. The short depth of field of the microscopes and a vertical cross-hair allowed detection of any significant rotation or translation of the specimen. Calibration of each microscope field was made using a Bausch and Lomb stage micrometer. Observation of a David Mann Co. glass scale permitted determination of the initial gauge length to within 5 μm, thus making the $\Delta l/l_0$ measurement absolute (except for specimen No. 1; see Sec. II). The error in Δl was somewhat larger than the micrometer least count of 0.5 μm. The principal error arose in judging the center of the markers as viewed through the rather irregular and changing surface of the refractive krypton (index 1.3).

D. X-Ray Lattice Expansion Measurements

The method employed determines $\Delta a/a_0$ with an uncertainty less than 12 ppm.[19] We emphasize here that the method is absolute and quite independent of the $\Delta l/l_0$ measurement.

II. RESULTS

We have mentioned above, and other workers have recently emphasized elsewhere,[20] the particular difficulties in the careful preparation and handling of noble-gas solids. It is therefore necessary to give a rather specific account of the present measurements.

Figure 3 presents the results of differential expansion measurements made on three krypton specimens. On specimen Nos. 1 and 2 length and lattice-parameter measurements were made over the entire range of temperatures, from 4 to 114°K. On specimens No. 2 and 3 only the extreme end, more than 5 mm (i.e., about the specimen diameter) below the lower markers, was in contact with the specimen tube. Figure 3 shows that measurements made on specimen No. 2 showed excellent agreement with the x-ray measurements for $T<75$°K. In addition, x-ray measurements for specimens No. 1 and 2 showed excellent agreement over the entire temperature range,[19] which proves that the temperature scale was reproducible. On specimen No. 3, only changes in length were measured and only for temperatures above 77°K. The smoothed values of $\Delta a/a_0$ measured on the previous two specimens were then used to find $(\Delta l/l_0-\Delta a/a_0)$ for specimen No. 3.

The length-change measurements made on specimen No. 1 are subject to some interpretation. The lower end of this specimen, including a portion near the lower markers, had become cemented to the specimen-tube wall by vapor deposition of krypton during the initial cooling of the specimen in a slight temperature gradient. The nature of the constraint was such that the length measurements were observed to be reversible over a sizable temperature interval. Figure 4 shows the observed length-change measurements on specimen No. 1 at the higher temperatures. The observed length between markers at 4.2°K was 75.727 mm. In view of the reversibility, it is reasonable to attempt to find an

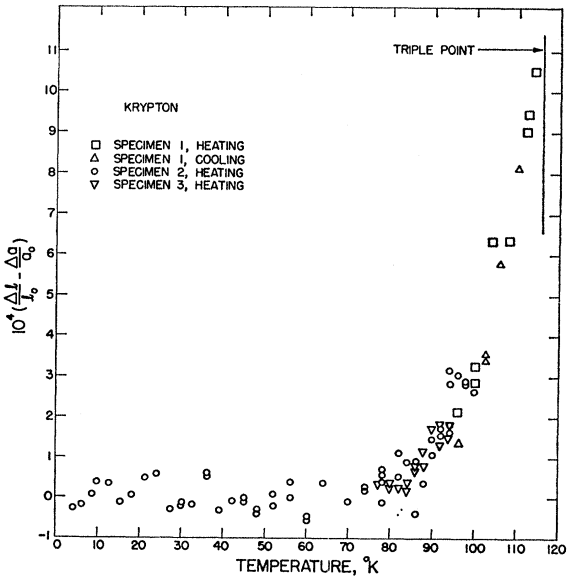

FIG. 3. Comparison of bulk length expansion measurements, $\Delta l/l_0$, with x-ray lattice expansion measurements, $\Delta a/a_0$, in solid krypton. The reference lengths are those values extrapolated to 0°K. The two measurements agree within 3×10^{-5} up to 75°K, at which $\Delta l/l_0=\Delta a/a_0=1604\times10^{-5}$.

[19] D. L. Losee and R. O. Simmons, following paper, Phys. Rev. 172, 944 (1968).

[20] A. Berné, G. Boato, and M. DePaz, Nuovo Cimento 46, 182 (1966).

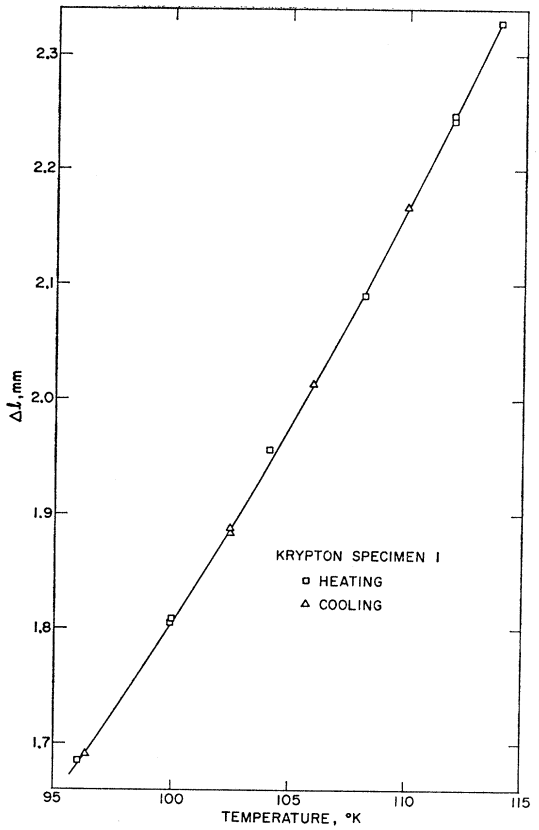

FIG. 4. Length-change measurements on krypton specimen 1 as discussed in text, Sec. II.

effective gauge length l_0 and to use this to determine the slope of $\Delta l/l_0$ at the highest temperatures. Such l_0 values were determined by comparing $\Delta a/a_0$ and $\Delta l/l_0$ over temperature ranges below which vacancy effects were evident in specimens No. 2 and 3. Fitting $\Delta l/l_0$ over a number of different temperature ranges consistently produced substantially the same variation for values of $(\Delta l/l_0-\Delta a/a_0)$ as a function of temperature. We therefore believe that some reliance may be placed upon such a fitting procedure. The results for the very highest temperatures, using the fitted value of $l_0=69.2$ mm, have been joined to the results of the measurements made on specimen No. 2 at 100°K. Because of the fitting procedure, we do not show the many $\Delta l/l_0$ values obtained for specimen No. 1 in the range below 100°K as independent data. The values exhibit the same degree of consistency as those of specimen No. 2 which are shown.

The quantity $(\Delta l/l_0-\Delta a/a_0)$ seems definitely to start differing from zero in the neighborhood of 80°K, reaching a value of 3.3×10^{-4} at 100°K. At 104°K, specimen No. 2 began moving inside the specimen tube, apparently as a result of slow mass transport of specimen material at the lower end of the specimen to other areas of the specimen tube. This movement, consisting of vertical sliding (at rates up to 1 μm/min) and some slight rotation, made further length measurements unreliable, and for that reason, measurements made on this specimen above 100°K have been disregarded.

Length measurements made on the third specimen at temperatures between 77 and 94°K (between which $\Delta l/l_0=66.8\times10^{-4}$) substantiate the results of the measurements made on specimen No. 2. Again mass transport via the vapor phase prevented precise measurements above 94°K.

The reversibility of the length measurements made on specimens No. 2 and 3 could not be verified because of the movement of the specimens just noted. However, the repeatability of the expansion measurements made on these two specimens lends credibility to the results. Furthermore, in spite of specimen motion, a large difference between the bulk and x-ray expansions of specimen No. 3 was noted in the neighborhood of 110°K. Although the value of $(\Delta l/l_0-\Delta a/a_0)$ observed at this point was less than what would be expected from the scaled data on specimen No. 1, it lends support to the validity of the results obtained by such a scaling. While there are many factors which may contribute to make measurements of $\Delta l/l_0$ too small, it is highly unlikely, in the present experimental arrangement, that any form of specimen constraint or other irreversible phenomenon could cause the $\Delta l/l_0$ measured on heating to be larger than the equilibrium values.

Relatively few x-ray measurements were made after cooling. Earlier extensive work on argon,[21,22] neon,[23] and krypton,[24] which involved both heating and cooling, showed that no difference would be expected in such a case.

III. THERMAL DEFECT PROPERTIES

A. Interpretation of $(\Delta l/l_0-\Delta a/a_0)$

The equilibrium atomic fraction n_j, of the jth type of atomic defect, at a given temperature and pressure is

$$n_j=K_j\exp(-g_j^f/kT)=K_j\exp(s_j^f/k)\exp(-h_j^f/kT), \quad (3)$$

where K_j is a geometrical factor ($=1$ for monovacancies) and g_j^f is the Gibbs free energy for the defect,

$$g_j^f=\epsilon_j^f+Pv_j^f-Ts_j^f. \quad (4)$$

The quantities ϵ_j^f, v_j^f, s_j^f, and h_j^f are the energy, volume, and vibrational entropy and enthalpy, respectively, associated with the formation of the defect at pressure P and temperature T.

If the concentration of equilibrium interstitial-type defects is assumed to be negligible, as indeed one would

[21] O. G. Peterson, D. N. Batchelder, and R. O. Simmons, Phil. Mag. **12**, 1193 (1965).
[22] O. G. Peterson, D. N. Batchelder, and R. O. Simmons, Phys. Rev. **150**, 703 (1966).
[23] D. N. Batchelder, D. L. Losee, and R. O. Simmons, Phys. Rev. **162**, 767 (1967).
[24] A. O. Urvas, D. L. Losee, and R. O. Simmons, J. Phys. Chem. Solids **27**, 2269 (1967).

expect in close-packed crystals,[25] then the extra relative number of thermally generated atomic sites is

$$\Delta N/N = n_1 + 2n_2 + 3n_3, \qquad (5)$$

where n_1, n_2, and n_3 are the atomic fractions of monovacancies, divacancies, and trivacancies, respectively. For purpose of discussion, we neglect any contributions due to quadrivacancies or larger clusters.

Figure 5 shows the results of plotting the measured values of $ln(\Delta l/l_0 - \Delta a/a_0)$ versus $1/T$. If an effective entropy of formation is taken to be approximately $2.0k$ (see Sec. III C) and a straight line is drawn through the data, then the effective vacancy enthalpy of formation is found to be $h^f/k = (895 \pm 100)$ deg, where k is the Boltzmann constant. We have taken these values to represent the vacancy concentrations in the following paper on thermal properties of solid krypton.[19]

The free energies of formation of the divacancy and trivacancy may be expressed as $g_2^f = 2g_1^f - g_2^b$ and $g_3^f = 3g_1^f - g_3^b$, where g_2^b and g_3^b are binding energies

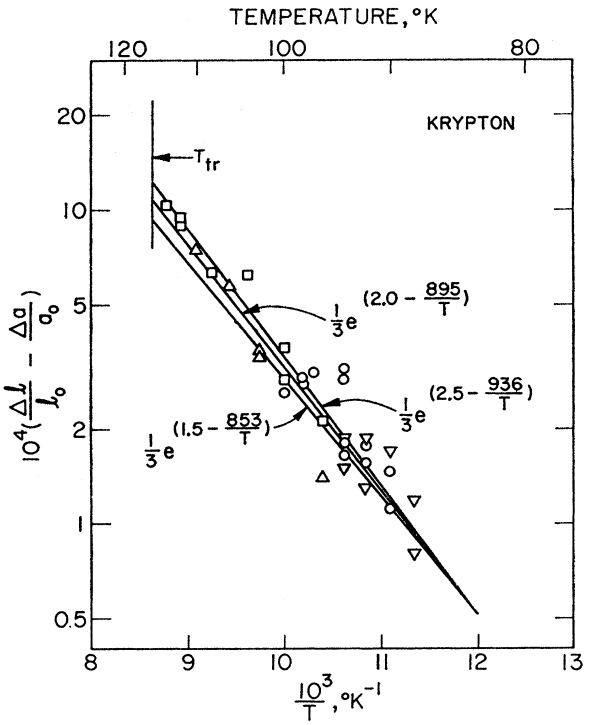

FIG. 5. Semilogarithmic plot of $(\Delta l/l_0 - \Delta a/a_0)$ versus reciprocal temperature to test for thermal defects in krypton, after Eq. (3). Data points are designated as follows: □, specimen 1, heating; △, specimen 1, cooling; ○, specimen 2, heating; ▽, specimen 3, heating. T_{tr} is the triple-point temperature.

[25] It was reported in Ref. 13, employing a truncated Morse potential and a static lattice approximation, that for such a model the interstitial energy of formation in krypton is about three times that of the monovacancy. In addition, we think it likely that the vibrational entropy of formation of the interstitial is smaller than that of the vacancy. (We note that in Ref. 13, an incorrect value was employed for the isothermal compressibility in fitting the potential parameters.)

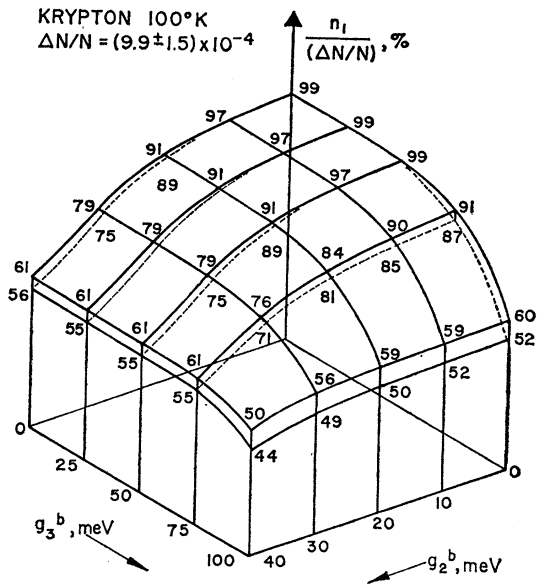

FIG. 6. Relative monovacancy abundance $n_1/(\Delta N/N)$ as a function of various divacancy and equilateral trivacancy binding free energies g_2^b and g_3^b, in solid krypton at 100°K. The upper and lower surfaces correspond to the lower and upper limits, respectively, on the measured $\Delta N/N$ value. The monovacancy free energy of formation, g_1^f, is about 68 MeV at 100°K.

associated with the divacancy and trivacancy, respectively. If the divacancy is taken to be two nearest-neighbor vacant atomic sites ($K_2 = 6$) and the trivacancy is taken to have the equilateral-triangle configuration ($K_3 = 8$), then one has

$$\Delta N/N = n_1 + 12n_1^2 \exp(g_2^b/kT) + 24n_1^3 \exp(g_3^b/kT). \qquad (6)$$

The fraction of vacant atomic sites which are monovacancies depends on the binding energies g_2^b and g_3^b. Solutions of Eq. (6) may be presented as the ratio $n_1/(\Delta N/N)$ versus the binding energies g_2^b and g_3^b; this is shown in Fig. 6 for krypton at 100°K. For a given set of values for the binding energies, the ratio is accurately given by the present $\Delta N/N$ data.

Multivacancy binding energies in noble-gas crystals have received little consideration in the literature.[11] A crude estimate consistent with the present work may be made, however. For the case of only short-range interaction between pairs and triples of atoms and in the absence of any lattice or electronic distortions, the divacancy binding energy would be

$$g_2^b = -(\tfrac{1}{6}E_2/N + \tfrac{1}{2}E_3/N), \qquad (7)$$

where E_2/N and E_3/N are the two-body and three-body contributions to the cohesive energy of the solid (see Sec. III B below). In the present case, this yields an approximate contribution of 15% to $\Delta N/N$ due to divacancy formation at 115°K, decreasing to 2% at 90°K.

A similar estimate for the trivacancy binding energy indicates only a negligible contribution to $\Delta N/N$ from trivacancy formation. Thus we estimate a monovacancy free energy of formation, $g_1^f=(77\pm8)$ MeV $-(2.0_{-0.5}^{+1.0})kT$, which is consistent with the measured value of $\Delta N/N$ and the first-order estimation of contributions due to vacancy clustering.

Finally, it is interesting to note that an empirical relation satisfied by fcc metals also appears to describe the maximum vacancy content in solid krypton, $(\Delta N/N)_m$. The relation[26] is

$$(\Delta N/N)_m \simeq (1/30)[(\Delta V/V)_m - 1/30]. \quad (8)$$

For krypton, the volume change on melting at the triple point is $(\Delta V/V)_m=12\%$, which yields $(\Delta N/N)_m \simeq 0.3\%$, in agreement with the present direct measurements. We do not think that this agreement implies that a "critical" concentration of vacancies is required for the melting of a fcc substance, because careful experiment has not detected any indication of vacancy premelting.[21,27] Rather, it appears possible that the interatomic forces which determine the vacancy free energy in a given fcc solid also determine the local structure of the liquid phase of that element.

B. Vacancy Enthalpy of Formation

Contributions to the vacancy enthalpy of formation, $h^f=\epsilon^f+Pv^f$, arise from several sources in noble-gas crystals. The major contribution to ϵ^f comes from the potential energy change of the crystal lattice when a crystal of N atoms occupying N atomic sites goes to a configuration having N atoms on $(N+1)$ sites. In the static rigid-crystal approximation the potential energy of the perfect crystal, relative to atoms separated at infinity, may be written

$$E_p=\frac{1}{2!}\sum_{i\neq j}\phi_{ij}+\frac{1}{3!}\sum_{i\neq j\neq k}\phi_{ijk}+\frac{1}{4!}\sum_{i\neq j\neq k\neq l}\phi_{ijkl}+\cdots, \quad (9)$$

where ϕ_{ij} is the two-body additive interaction potential between the ith and jth atoms and ϕ_{ijk} is the pairwise-nonadditive contribution to the interaction energy of the ith, jth, and kth atoms. For brevity in further discussion, we shall omit higher-order terms in Eq. (9), although there is at present no firm evidence to show that this multibody series shows rapid convergence.[28] The crystal is taken to be large enough so that the fraction of surface atoms is negligible. To this order of interaction, the cohesive energy per atom can be written

$$\frac{E_p}{N}=\frac{1}{2!}\sum_{1\neq j}\phi_{1j}+\frac{1}{3!}\sum_{1\neq j\neq k}\phi_{1jk}=\frac{E_2}{N}+\frac{E_3}{N}. \quad (10)$$

On the other hand, removal of one atom from within the crystal to infinity requires an energy

$$E_\infty=-\sum_{1\neq j}\phi_{1j}-\frac{1}{2!}\sum_{1\neq j\neq k}\phi_{1jk}. \quad (11)$$

The subsequent return of this atom to the surface of the crystal (without change of the surface configuration) is accompanied by an energy release $|F_p/N|$ since the energy of the crystal is required to be a homogeneous function of N. (Alternatively, one may think of the entire crystal being constructed, one atom at a time, by a succession of such processes.) Hence the energy of formation of a monovacancy in the static rigid lattice is

$$\epsilon^f=-E_\infty+E_p/N=-E_p/N-E_3/N. \quad (12)$$

The neglected terms in Eq. (9) would contribute similar terms to Eq. (12).

Thus we see that the difference between ϵ^f and the cohesive energy per atom is a measure of the many-body interaction in such a rigid crystal. Additional contributions to ϵ in the real crystal arise from lattice and electronic relaxations. The possible magnitudes of these various quantities evidently require our consideration next.

Our measured enthalpy, $h^f=77$ MeV, is essentially equal to ϵ^f at the saturated vapor pressure, if v^f is no larger than two atomic volumes.[19] This is significantly less than an average value of $-E_p/N$,[15] obtained from calorimetric and vapor-pressure data, of (120+1.3) MeV.

Most theoretical calculations of vacancy properties in the noble-gas solids have been done for the case of argon. In Table I we summarize the results obtained by a number of workers. Though there is apparently a wide degree of disagreement in some cases regarding the vacancy properties in argon, we shall here try to use these calculations to make some inferences about the properties of vacancies in krypton.

First we note that the calculations of relaxation energy predict a relatively small energy associated with the relaxation of the *lattice* about the vacant site, usually of the order of 2% of the cohesive energy per atom. No independent value of this relaxation is available from experiment, because the equal relaxation contributions to $\Delta a/a$ and $\Delta l/l_0$ are cancelled when $\Delta N/N$ is obtained from Eq. (2). We note that such a small relaxation is not inconsistent, however, with the observed temperature variation of the thermal properties of krypton.[19] Carrying a 2% figure to the case of krypton, we may tentatively estimate a lowering of h^f by about -3 MeV due to the lattice relaxation.

[26] R. O. Simmons, J. Phys. Soc. Japan 18, Suppl. II, 172 (1963).
[27] D. R. Beaman, R. W. Balluffi, and R. O. Simmons, J. Chem. Phys. 41, 2791 (1964).
[28] H. Margenau and J. Stamper, in *Advances in Quantum Chemistry*, edited by P. Löwdin (Academic Press Inc., New York, 1967), Vol. III, p. 129. See also E. Lombardi and L. Jansen Phys. Rev. 167, 822 (1968).

TABLE I. Calculations of properties of monovacancies in solid argon. $|E_p|$ is the potential energy per atom in the crystal (taken to be 79.6 MeV for argon). E is the sum of all additional terms contributing to the vacancy energy of formation ϵ^f. (v^f-v_a) is the relaxation volume associated with the vacancy, where v_a is the atomic volume in the crystal. s^f is the vibrational entropy of formation.

Reference	$E/\|E_p\|=(\epsilon^f/E_p)-1$	$(v^f-v_a)/v_a$	s^f/k	T, °K	Remarks
a	−0.004	−0.02	···	0	Lattice statics model, central forces
b	−0.018	−(small)	···	0	Static model, 12-6 potential
c	···	+0.02	2.3	80	Dynamic model, 12-6 potential
d	−0.45	···	···	0	Three-body electron exchange model
e	−0.40 [f]	−0.24	···	0	Static model, including three-body forces
g	−0.002	+0.05 [h]	···	80	Dynamic model, 12-6 potential
i	$\epsilon^f/k=116$ MeV [j]	+0.73	8.1	80	Dynamic model, central forces
k	−0.21	···	···	···	Electron shell model
l	−0.13	+(small)	···	0	Static model, 12-6 potential
m	−0.02	+(small)	4.0	80	12-6 potential, see text, Sec. III C
n	−0.02	−0.08	···	0	Static model, Morse potential
o	+0.10	+0.06	4.78	···	Quasithermodynamic approximation
p	···	···	1.5+	···	General rigid lattice model

[a] Reference 2.
[b] Reference 3.
[c] Reference 4.
[d] Reference 5.
[e] Reference 6.
[f] Of this amount only −0.02 was elastic (lattice) relaxation energy.
[g] Reference 8.
[h] This value has been obtained from the asymptotic behavior of the relaxation by means of continuum theory.
[i] Reference 9.
[j] These authors appear to have considered the energy required to remove an atom from the lattice to a point infinitely far from the crystal.
[k] Reference 10.
[l] Reference 11.
[m] Reference 12.
[n] Reference 13.
[o] Reference 14.
[p] Reference 35.

The electronic relaxation energy may be somewhat larger than the lattice relaxation energy. Through a sum-rule analysis of index of refraction data and exciton absorption spectrum data for argon, Doniach and Huggins[10] estimated a contribution to h^f equal to $0.1|E_\infty|$ due to polarization of the atoms surrounding the vacant site. These authors noted, however, that their result for this relaxation energy is rather sensitive to the parameters in their model. Index of refraction data are now available for krypton[29] but a similar calculation for the vacancy has not yet appeared. Carrying the rough 10% figure over to krypton leads to a possible electronic contribution to h^f of −24 MeV.

Thus, using Eq. (12), and the approximate relaxation corrections noted below it, we estimate the many-body contribution to the potential energy of solid krypton to be $(+16_{-9}^{+13})$ MeV. The stated limits of uncertainty are an attempt to include contributions both from possible errors in our measurements and from uncertainties in the corrections.

The value ∼16 MeV (∼375 cal/mole) is consistent with recent calculations for the triple-dipole interaction,[30,31] or with calculations of three-body exchange energy,[5] which are similar in magnitude. We therefore cannot discriminate between various possibilities for the origin of the many-body force contributions nor assign their importance relative to one another.

There has been considerable discussion in the literature[28,32,33] concerning the possible magnitude of many-body effects in the noble-gas solids. However, few experimental quantities have been available which are sensitive to the presence of many-body forces. Generally, the bulk scalar properties can give little direct information about such effects. The microscopic and tensor properties of the solid, however, are much more sensitive to many-body effects. It was shown above that the vacancy energy of formation gives a measure of the three-body energy. An earlier experimental examination of this question by Peterson and co-workers,[21] using Eq. (1), showed that no definite conclusion could be reached about the necessity of many-body forces, with the inaccurate bulk density data then available. The elastic stiffnesses c_{ij} may provide information on the spatial dependence of the many-body forces. Unfortunately, no single-crystal elastic data for krypton are presently available, and published phonon dispersion relations[34] are insufficiently accurate for small wave numbers to yield elastic data. Until further measurements have been made, the precise magnitude of the many-body interactions in the noble-gas solids will remain somewhat a matter of conjecture.

C. Vacancy Entropy of Formation

A value for the vibrational entropy of formation of a vacancy in an otherwise perfect lattice having harmonic interactions between nearest-neighbor atoms has been calculated in first order to be $s^f=\frac{3}{2}k$.[35] One expects that lattice relaxations and interactions between vacancies may modify this value in the direction of

[29] A. C. Sinnock and B. L. Smith, Phys. Letters **24A**, 387 (1967).
[30] W. Götze and H. Schmidt, Z. Physik **192**, 409 (1966).
[31] A. Lucas, Physica **35**, 353 (1967).
[32] A varied record of current views about multibody interatomic forces in the condensed state, with many references, appears in Discussions Faraday Soc. **40**, (1965).
[33] C. E. Swenberg, Phys. Letters **24A**, 163 (1967); this author points out an apparent lack of self-consistency in Jansen's treatment of three-body interactions. A rebuttal is given by L. Jansen and E. Lombardi, Chem. Phys. Letters **1**, 33 (1967).
[34] W. B. Daniels, G. Shirane, B. C. Frazer, H. Umebayashi, and J. A. Leake, Phys. Rev. Letters **18**, 548 (1967).
[35] K. F. Stripp and J. G. Kirkwood, J. Chem. Phys. **22**, 1579 (1954).

increasing the entropy of formation. Also, calculations on a high-temperature anharmonic model have given $s^f \simeq 2k$.[36] In the case of fcc metals, the monovacancy entropy of formation has been found experimentally to be relatively close to $2k$.[26]

Because of the long extrapolation required to reach $1/T=0$ in Fig. 5, there is a range of s^f values which might be deduced in the light of the relatively uncertain nature of the high-temperature expansion measurements made on specimen No. 1. The value selected, $s^f=(2.0_{-0.5}^{+1.0})k$, seems to fit the data best and also is reasonable compared with the known entropies of formation for vacancies in close-packed metals.

Values of s^f much greater than $\frac{5}{2}k$ do not appear to be consistent with the observed values of $\Delta N/N$. The upper line drawn in Fig. 5, with $s^f=\frac{5}{2}k$ and $h^f=81$ MeV, seems to be a good approximation to the measured $\Delta N/N$ values which must include contributions due to the formation of divacancy and trivacancy clusters at the higher temperatures. Further, some rather indirect support for the chosen value of s^f comes from comparison of the present h^f value with the value of h^f deduced by Beaumont and co-workers[16] by analysis of specific-heat data for krypton. Their analysis gave $h^f=(77\pm9)$ MeV. If a higher value of s^f were chosen in the present work, we would be led to substantially higher values of h^f.

If the enthalpy of formation is a temperature-dependent quantity and is expanded in a series as a function of temperature,

$$h^f=h^0+h'T+h''T^2\cdots, \tag{13}$$

the leading term in the temperature-dependent part of h^f will contribute to the free energy in the same way that an entropy term contributes. In a recent calculation Glyde[12] obtained a value for s^f in solid argon of $4k$. This rather large entropy is due to the temperature dependence of the lattice potential energy for his model. His model is not self-consistent, however. The calculation used a Mie-Lennard-Jones 12-6 potential fitted to a harmonic model at $T=0$°K and the experimental values of the lattice parameter as a function of temperature.[21] The temperature dependence of ϵ^f seems to be rather sensitive to the analytic form of the interatomic potential used in such a calculation if experimental data are used to determine the volume at a given temperature.

The specific-heat analysis of Beaumont and co-workers[16] is insensitive to the value of the coefficient h' as defined by Eq. (13). The agreement of the present value of h^f with the calorimetric analysis and the apparent rather low entropy associated in the present work with this figure tend to indicate only a rather weak temperature dependence for h^f.

[36] J. Mahanty, A. A. Maradudin, and G. W. Weiss, Progr. Theoret Phys. (Kyoto) 24, 648 (1960).

D. Self-Diffusion in Krypton and a "Law of Corresponding States"

Self-diffusion in most close-packed solids is governed by the presence and migration of vacant atomic sites. The self-diffusion coefficients in argon[20] and xenon[37] have been found to follow a relation of the form $D=D_0\times\exp(-q/kT)$. For a monovacancy mechanism, the activation energy is $q=\epsilon^f+\epsilon^m$, where ϵ^m is the energy of migration of the vacancy. The preexponential factor is $D_0=a^2\nu\exp(s^f/k+s^m/k)$, where s^m is the vibrational entropy of migration of the vacancy and ν is a frequency factor including correlation effects.

A law of corresponding states has been found to describe a number of thermostatic properties of the noble-gas solids at temperatures near their triple points (see, for example, Refs. 19 and 24). Also, consideration of corresponding-states relations have been extended to transport properties in the condensed state of these substances by Rice and co-workers.[38] Consequently, one expects that values for q and ϵ^f for each of the noble-gas solids may be proportional to the triple-point temperature T_{tr} (or to an energy parameter in an interatomic potential function). Table II shows the results obtained from such a scaling procedure applied to the heavy noble-gas solids.

First, the ratio q/kT_{tr} is indeed very nearly the same for argon and xenon. The value 23.0 for this ratio may then be chosen to predict $q/k=2660$°K for krypton.

Second, one may apply the same empirical procedure to predict vacancy formation energies in the other solids. The value for argon, $\epsilon^f/k=640$°K, is strikingly similar to the value obtained by Beaumont and co-workers[16] from analysis of specific-heat data, $\epsilon^f/k=(640\pm65)$°K. If one further adopts a value for argon of $s^f\simeq2k$, then the predicted vacancy content at its triple point is 0.35%. Independent evidence about this number for argon is available through the application of Eq. (1) with the known x-ray density[21] but, as pointed out above, the bulk data are rather inaccurate. From

TABLE II. Experimental and predicted activation energies for self-diffusion q and vacancy formation ϵ^f in the heavy noble-gas solids. Quantities in parentheses are predicted by a law of corresponding states. T_{tr} is the triple-point temperature. The measured ϵ^f value for krypton corresponds to $E/|E_P|=-(0.36\pm0.07)$, for comparison to Table I.

Element	q/k, °K	q/kT_{tr}	ϵ^f/k, °K
A	1940 ± 100 [a]	23.2 ± 1.2	(640)
Kr	(2660)	(23.0)	895 ± 100 [b]
Xe	3710 ± 25 [c]	23.0 ± 0.2	(1250)
Rn	(4650)	(23.0)	(1520)

[a] Tracer diffusion, Ref. 20.
[b] Present work.
[c] NMR measurements, Ref. 37.

[37] W. M. Yen and R. E. Norberg, Phys. Rev. 131, 269 (1963).
[38] See, for example, J. Naghizadeh and S. A. Rice, J. Chem. Phys. 36, 2710 (1962).

bulk density measurements, Smith and Chapman[39] give a value $\leq 0.13\%$; while from P-V-T measurements, van Witzenburg[40] gives $(0.37\pm 0.25)\%$. The latter value is closer to an empirical prediction for argon using Eq. (8).

Because of the relatively large uncertainties in the preexponential factor D_0, no empirical prediction of D_0 for krypton can be made. The tracer diffusion measurements on argon[20] result in values of D_0 which differ by more than an order of magnitude. Further, there appears to be 40% uncertainty in D_0 as deduced from NMR experiments on xenon.[37] Within the uncertainties, values of D_0 can be adopted in agreement with expectation for fcc substances.[20] We note that a classical law of corresponding states is not strictly suitable for such properties as compressibility[24] and coefficient of thermal expansion.[19] Similarly, some influence of the zero-point motion upon D_0 may be expected.

In the noble-gas solids the presence of appreciable divacancy concentrations (Sec. III A above) may lead to significant divacancy contributions to the self-diffusion. For a nearest-neighbor divacancy model, the ratio of tracer diffusivities is[26]

$$D_2/D_1=(2\nu_2/3\nu_1)(n_2/n_1)\exp[(g_1^m-g_2^m)/kT], \quad (14)$$

where $g^m=h^m-Ts^m$ and the frequency factors ν include correlation effects. In several fcc metals, the exponential factor is observed to be of order unity; but in argon, only a rudimentary theoretical study of some aspects of this problem has been published.[11]

Comparison of observed self-diffusion with theory for argon reveals two calculations which claim agreement.[11,12] The calculations consist of evaluation, for a given model, of individual quantities such as ϵ^f, ϵ^m, and so on. If the present measurements of vacancy concentration and their interpretation are correct, then both such apparent agreements of theory are fortuitous and depend upon compensating errors in the calculations.

IV. CONCLUSION

The determination of vacancy properties in the noble-gas solids may provide important information concerning the nature of the forces acting in these solids. While much theoretical work has been done in this area, the present experimental data indicate that more refined theoretical calculations are needed. The present value of vacancy enthalpy is significantly different from the potential energy per atom, in disagreement with most theoretical models. Of particular interest is the problem of electronic relaxation energy associated with a vacancy. This problem in turn has a bearing on the magnitude of the many-body forces in these solids.

The relatively large fraction (up to 0.3%) of atomic vacancies in krypton and probably in the other noble-gas solids near their triple points may have important effects on other properties of these solids.

---

[39] B. L. Smith and J. A. Chapman, Phil. Mag. **15**, 739 (1967).
[40] W. van Witzenberg, Phys. Letters **25A**, 293 (1967). See also W. van Witzenberg and J. C. Stryland, Can. J. Phys. **46**, 811 (1968).